Review

A review of deep learning approach to predicting the state of health and state of charge of lithium-ion batteries

Kai Luo [a], Xiang Chen [b], Huiru Zheng [c,*], Zhicong Shi [a,*]

[a] School of Materials and Energy, Guangdong University of Technology, Guangzhou 510006, Guangdong, China
[b] Department of Chemical Engineering, Tsinghua University, Beijing 100084, China
[c] School of Computing, Ulster University, Belfast BT15 1ED, United Kingdom

ARTICLE INFO

ABSTRACT

In the field of energy storage, it is very important to predict the state of charge and the state of health of lithium-ion batteries. In this paper, we review the current widely used equivalent circuit and electrochemical models for battery state predictions. The review demonstrates that machine learning and deep learning approaches can be used to construct fast and accurate data-driven models for the prediction of battery performance. The details, advantages, and limitations of these approaches are presented, compared, and summarized. Finally, future key challenges and opportunities are discussed.

© 2022 Science Press and Dalian Institute of Chemical Physics, Chinese Academy of Sciences. Published by ELSEVIER B.V. and Science Press. All rights reserved.

Kai Luo obtained his Bachelor's degree from Guangdong University of Technology in 2020. He is an MSc student under the supervision of Prof. Zhicong Shi at the School of Materials and Energy, Guangdong University of Technology. His current research interests focus on the interdisciplinary research of deep learning and lithium-ion batteries.

Huiru Zheng received her BSc, MSc, PhD degrees from Zhejiang University, Fuzhou University and the University of Ulster, UK in 1989, 1992 and 2003 respectively. Her research area includes data mining, machine learning, artificial intelligence, and their applications. She has published over 330 research papers in peer reviewed international journals and conferences. Dr. Zheng is currently a Professor of Computer Science and AI Research Centre Theme Lead with the School of Computing at Ulster University, UK.

Xiang Chen gained his Bachelor's and Ph.D. degrees from the Department of Chemical Engineering at Tsinghua University in 2016 and 2021, respectively. He is currently a Shuimu Tsinghua Scholar at Tsinghua University. His research interests focus on understanding the chemical mechanism and materials science in rechargeable batteries mainly through multi-scale simulations and machine learning.

Zhicong Shi received his Ph.D. degree in Physical Chemistry from Xiamen University in 2005. He joined the Dalian University of Technology as an associate professor after a postdoctoral fellowship from the University of Alberta, Canada. Now, he is a professor at the School of Materials and Energy, Guangdong University of Technology. His current research interests focus on design, characterization, and understanding of the working mechanism of materials for supercapacitors, batteries, and fuel cells.

* Corresponding authors.
  E-mail addresses: h.zheng@ulster.ac.uk (H. Zheng), zhicong@gdut.edu.cn (Z. Shi).

1. Introduction

Climate change and the increasing global energy demands provide a strong impetus for the energy transition. As one of the most essential components, lithium-ion batteries (LIBs) are more and more crucial in changing the energy consumption structure and electrifying traditional energy sources [1,2]. LIBs have the advantages of high energy density, high charging efficiency, wide operating temperature, and long cycle life, so they have been widely used in energy storage power stations, consumer electronics and electric vehicles. But how to accurately model degradation behavior during operation is emergent [3-6]. It is a daunting challenge to accurately assess the health of the battery in use because of the complex degradation mechanisms [7,8].

The battery management system (BMS) indicates battery status and optimizes battery behavior, which can not only ensure the safety and remaining mileage of the vehicle within the lifespan of the battery but also ensure the daily normal operation of energy storage power stations [9–11]. BMS can collect battery status, analyze battery status, manage thermal, manage energy, protect the safety, *etc.* [12]. The most critical part is the algorithm model of data in the lifetime of batteries. The crucial is how to estimate the state of charge (SOC) and the state of health (SOH) to ensure the consistency of the battery pack during the charging and discharging process [13–15]. Recently, estimating the vehicle's remaining mileage becomes very popular. While obtaining SOC and SOH, the reliable prediction of the remaining useful life (RUL) can ensure users' safety, extend battery life, and maximize battery potential before the end of life [16]. Waste batteries with less than 80% useful life can still be used for second-life applications in some places with low requirements after being screened [17–19]. The calculation method of SOC and SOH is shown in Eqs. (1) and (2).

$$SOC = \frac{C_{curr}}{C_{full}} \times 100\% \tag{1}$$

$$SOH = \frac{C_{full}}{C_{nom}} \times 100\% \tag{2}$$

In Eq. (1), C_{curr}, C_{full}, and C_{nom} represent the battery capacity of the current state, the battery capacity of the fully charged state, and the nominal battery capacity of the brand-new state, respectively.

Conventional SOC estimation methods include but are not limited to the ampere hour counting or coulomb counting [20,21], open circuit voltage estimation [22,23], and Kalman filters [9,24,25]. The ampere hour counting calculates quickly and estimates immediately, but the error will be accumulated continuously. The open circuit voltage operates easily, but cannot be monitored in real time. SOC can only be obtained under long-term standing conditions. The Kalman filter uses non-linear calculations, and estimates better on the SOC, but which is suitable or not has a greater impact on the accuracy and precision of the SOC, and the computational cost is higher. For ease of reference, the definitions of abbreviations and acronyms used in this paper are listed in Table 1.

The SOC and SOH estimations develop quickly in recent years, but the relationship between computational efficiency and accuracy is irreconcilable. Recently, machine learning (ML) methods have been successfully applied in many fields since they do not require a deep understanding of priori knowledge [26–30]. In order to estimate the SOC and SOH of LIBs, there are traditional model-based methods such as the electrochemical model and the equivalent circuit model, as well as data-driven methods such as decision tree (DT), convolutional neural network (CNN), and recurrent neu-ral network (RNN). These methods have been used for estimating the battery SOC and SOH, and predicting the RUL in many works [25,26,31–43].

Interdisciplinary is the general trend. For traditional engineering disciplines like LIBs, trial-and-error methods are commonly used but inefficient. There is no doubt that the multidisciplinary cross has an empowering effect on traditional engineering, which provides an integrative study of the problem for the wider society. From the perspective of practitioners in the LIBs field, we hope to identify the commonalities among them and provide some suggestions for improving the development of prediction in LIBs usage status. Fig. 1 illustrates the framework of the BMS health diagnostics and prognostics algorithm.

In this paper, we review the applications of ML and deep learning (DL) in the estimation of the SOH and SOC of batteries in the last five years, and then discuss in detail the main factors that could have an impact on the prediction accuracy. In addition, issues such as the model complexity and the hyperparameter optimization involved in DL are also discussed. Since the recent advanced DL has the advantages in automatic features extraction and attractive prediction performance, this review will focus on the application of DL in predicting the SOH and SOC of LIBs. The remainder of the paper is organized as follows: Section 2 briefly introduces the traditional model-based approaches. Section 3 provides a detailed summary and discussion of the data-driven methods, including a brief review of traditional ML methods and an in-depth review of DL methods, in the prediction of SOC and SOH of LIBs. Section 4 provides a conclusion and outlook of DL in the SOH and SOC research area.

2. Model-based approaches

The core element of BMS is the battery model. The quality of models determines the battery pack can whether operate safely and guarantee its service life or not. In order to estimate the SOC and SOH of LIBs and predict the RUL, there are traditional model-based methods such as the electrochemical model and the equivalent circuit model [44–51].

2.1. Electrochemistry models

The electrochemical model of LIBs starts from the internal electrochemical mechanism of the battery, based on the theory of porous electrodes and concentrated solutions, through Ohm's law and Butler–Volmer kinetic equation, *etc.* The state and behavior of lithium ions in the battery such as physics and chemistry reaction processes are described by partial differential equations. The earliest electrochemical model is the quasi-two-dimensional model, which provides a comprehensive and systematic description of battery charging and discharging characteristics. Other models include single-particle models and simplified quasi-two-dimensional models (Fig. 2). Because the electrochemical model requires a lot of calculations, there are great limitations when applied to BMS [44–46].

2.2. Equivalent circuit models

The equivalent circuit model is the most mature and widely used online SOC estimation model in electric vehicles currently, which has characteristics of simple calculation and real-time prediction. It simulates the nonlinear characteristic parameters of LIBs through circuit elements with linear changes in parameters. Typical equivalent circuit models are Thevenin, PNGV, Rint, Randles, and GNL models. Equivalent circuits with higher orders have higher simulation accuracy. Although the computational efficiency

Table 1
Definitions of abbreviations and acronyms used in this paper.

Abbreviation	Term	Abbreviation	Term
LIBs	Lithium-Ion Batteries	LR	Linear Regression
BMS	Battery Management System	GPM	Gaussian Procession Model
SOC	State of Charge	SVM	Support Vector Machine
SOH	State of Health	LSTM	Long Short-Term Memory
RUL	Remaining Useful Life	EIS	Electrochemical Impedance Spectroscopy
ML	Machine Learning	DNN	Deep Neural Network
DT	Decision Tree	GRU	Gated Recurrent Unit
CNN	Convolutional Neural Network	TL	Transfer Learning
RNN	Recurrent Neural Network	AI	Artificial Intelligence
DL	Deep Learning		

is high, the accuracy of the equivalent circuit model is relatively limited [47–50]. The advantages and disadvantages of the two model-based methods are shown in Table 2.

2.3. Empirical models

The empirical model is based on historical data and is established by analyzing the correlation of numerous data. It is a simple model which doesn't concern the battery mechanism. It can establish the relationship between RUL and battery characteristics. In the process of using, the model parameters depend on historical data. If the accuracy of parameter identification is to be guaranteed, limited historical data should be paired with fewer parameters. If the data is sufficient, a model with more parameters is better. Kalman filters and particle filters are currently the most used parameter estimation methods. Kalman filters are recursive filters, including a prediction step and an update step, which is suitable for processing time-varying linear systems. Particle filters have the advantage in most nonlinear problems, so it is more appropriate to deal with the problem of battery RUL prediction [51]. The result of using the intelligent adaptive extended Kalman filter to estimate SOC and its error is shown in Fig. 3.
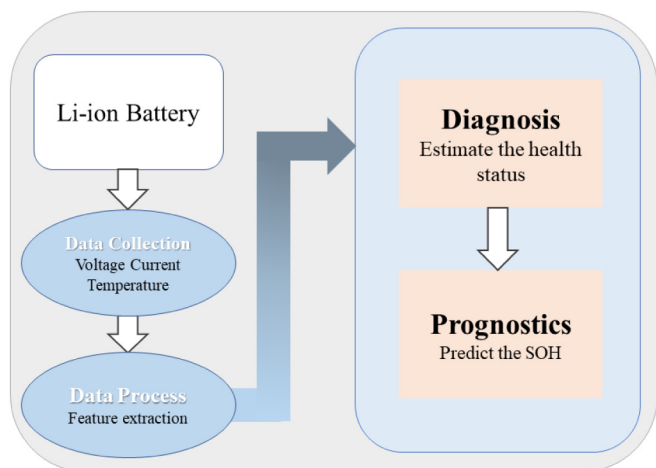

Fig. 1. BMS health diagnostics and prognostics algorithm framework.

3. Data-driven methods

3.1. Machine learning

The data-driven method, which uses historical data to describe the relationship between a lot of variables, has attracted wide attention recently [52,53]. ML becomes more and more important because of its great potential of low computing cost and high accuracy [15]. The data-driven method does not rely on the mechanism of LIBs. By establishing a mathematical model and inputting the relevant data, an ML model can be used to predict SOH or SOC after training. The common ML (also call shallow learning) models are linear regression (LR), gaussian procession, support vector machine (SVM), DT, which can be applied to optimization, prediction, and pattern recognition. ML has been used to predict LIBs after training on experimental data.

3.1.1. Linear regression

LR uses regression analysis to determine the quantitative relationship of dependence among multiple variables [54]. Because many batteries show nonlinear behavior, the method can be extended to nonlinear by adding quadratic or higher order terms in the fitting.

Severson et al. [39] used a linear model to predict the RUL of $LiFePO_4$ batteries after 100 cycles by cycle number, current, voltage, and capacity, with an error of 9.1%, which can predict the RUL accurately through the feature engineering of early data. Compared to using a single model, good performance can also be obtained by stacking. Aims to predict the capacity degradation, Liu et al. [55] proposed a strategy for LIBs of conventional layered oxide cathode by multivariate linear regression and discharge-voltage-related features.

3.1.2. Gaussian procession models

Gaussian procession model (GPM) is a stochastic method, which can provide predicted probability distribution and is defined by its covariance function and mean function [56,57].

Traditional methods of LIBs prediction rely on microscopic degradation mechanisms, such as the change of solid electrolyte interfaces [58,59], lithium plating [60,61], and active material loss [62,63]. Zhang et al. [36] combine electrochemical impedance spectroscopy (EIS) with the GPM to prove the value of the EIS signal in BMS. Through the fusion of multiple models and accounting for regeneration phenomena, Liu et al. [41] used GPM to capture the local fluctuations, and predicted the capacity one or more steps in advance by the LSTM-GPM. Different from others that only consider the internal characteristics and external performance changes of the battery during use, Yang et al. [64] proposed a GPM based on charging. Four specific parameters extracted from the charging curve are used as inputs to a GPM. In addition, the GPM is improved from the input variables, and grey correlation analysis is applied to analyze the correlation between the selected features and SOH. Capacity prediction results by different models are shown in Fig. 4.

3.1.3. Support vector machine

SVM classifies and regresses data by supervised learning, which has advantages in solving the problem of small samples, nonlinear, and high dimensional pattern recognition.

Nuhic et al. [37] propose a method of support vector regression for predicting RUL. The method can predict RUL by using the data of actual road condition batteries. In addition to regression attributes, SVM can also implement classification tasks. Meru et al. [65] proposed a method to integrate support vector classification and regression attributes, that is, to use SVM to build key features,
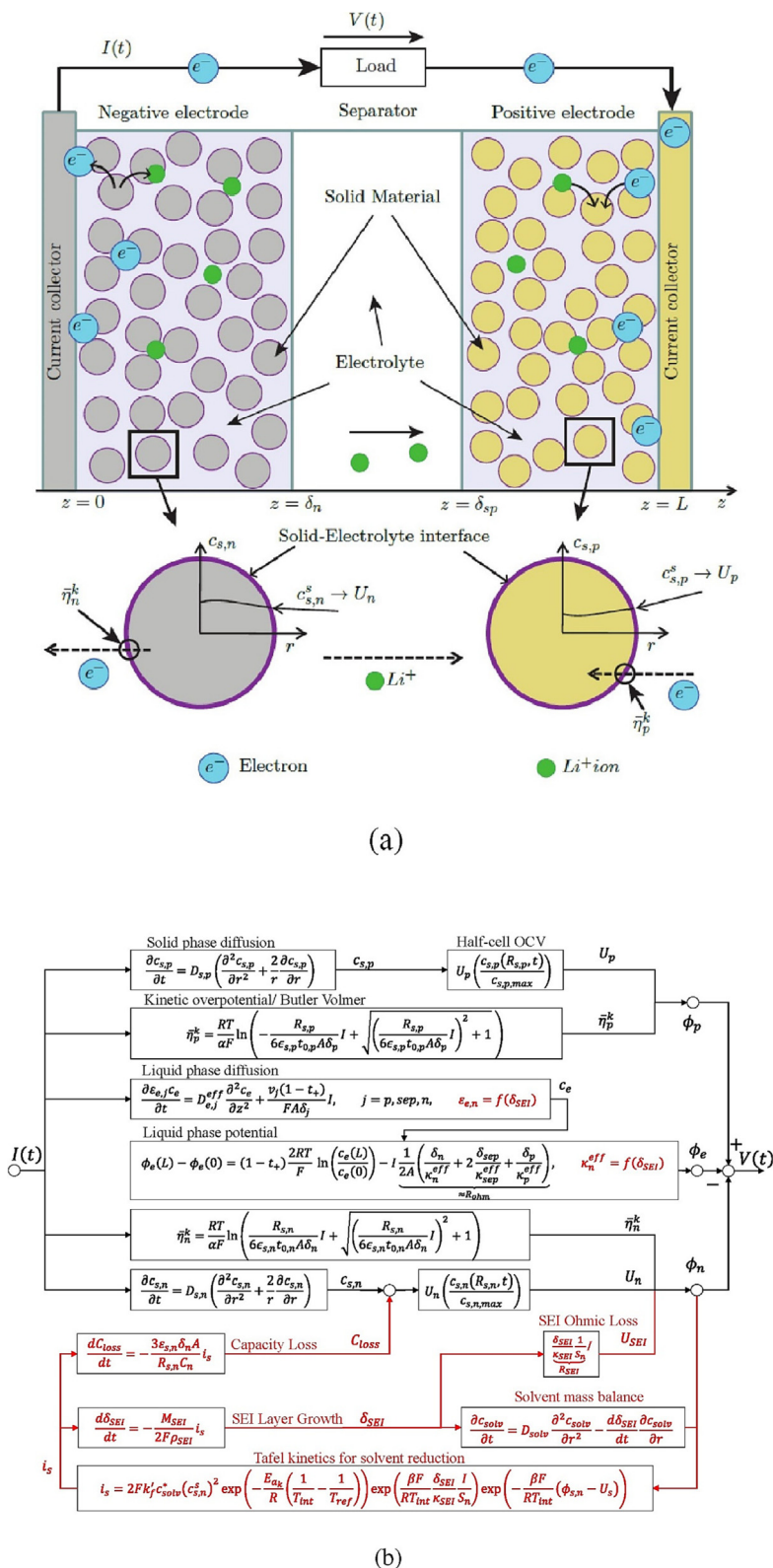
(a)

(b)

Fig. 2. Schematic diagrams of (a) derivation of a single particle model, (b) basic electrochemical equations (top, black) including aging extension (bottom, marked in red). Reproduced from Ref. [44] with permission from Elsevier.

and when the battery is near the service life, it uses support vector return to predict RUL. Combined with the engineering techniques in the experimental process, for example, thermal imaging is also a research method. Zhou et al. [66] proposed a method combining artificial neural networks and SVM with thermal imaging technology.

To solve the problem of most of the existed works focus on the long-term features in the battery degradation process, which are not easy to be obtained, Meng et al. [67] used the correlation between battery parameters and the response characteristics of terminal voltage to battery aging to propose a method to estimate the SOH by SVM. The method uses the terminal voltage response

Table 2
Comparison of model-based methods.

Property	Electrochemistry model	Equivalent circuit model
Advantages	Bases on the internal electrochemical process High accuracy	Describe changes in internal resistance
Disadvantages	Requires electrochemistry expert knowledge Difficult to find suitable model parameters	Expensive test equipment Electrochemical impedance spectroscopy test causes battery aging

characteristics of LIBs under the current pulse test, and the measured end voltage under the same condition will change when aging.

3.1.4. Decision tree

DT is a simple but widely used classifier. Constructing a DT through training data can efficiently classify and regress unknown data.

Through two aspects of the initial state (represented by the data of the first cycle) and the changing trend (by comparing the difference between the corresponding data in the second cycle and the first cycle), Zhu et al. [68] constructed the characteristics of the data and use the DT as the model, and finally achieve an accuracy of 95.2% when predicting the LIBs lifespan.

To solve the issue of overfitting, Zhang et al. [69] proposed a gradient boosting DT-based model, which selects features from the original data obtained during the charging and discharging process, then uses the correlation coefficient and DT to filter the features and uses the variance inflation factor to further filter to filter out effective features from the original battery information.

3.1.5. Brief summary

LIBs are accompanied by many measurable data during operation, such as current, voltage, impedance, time, and capacity. The more types of data, the greater the quantity, which means the richer the information, so it is reasonable that the performance of multi-variable and multi-battery data will be better. But ML tends to get more tractable, fixed-length inputs and outputs. Through feature engineering, better data features can be extracted from the raw data to promote the training effect. For structured
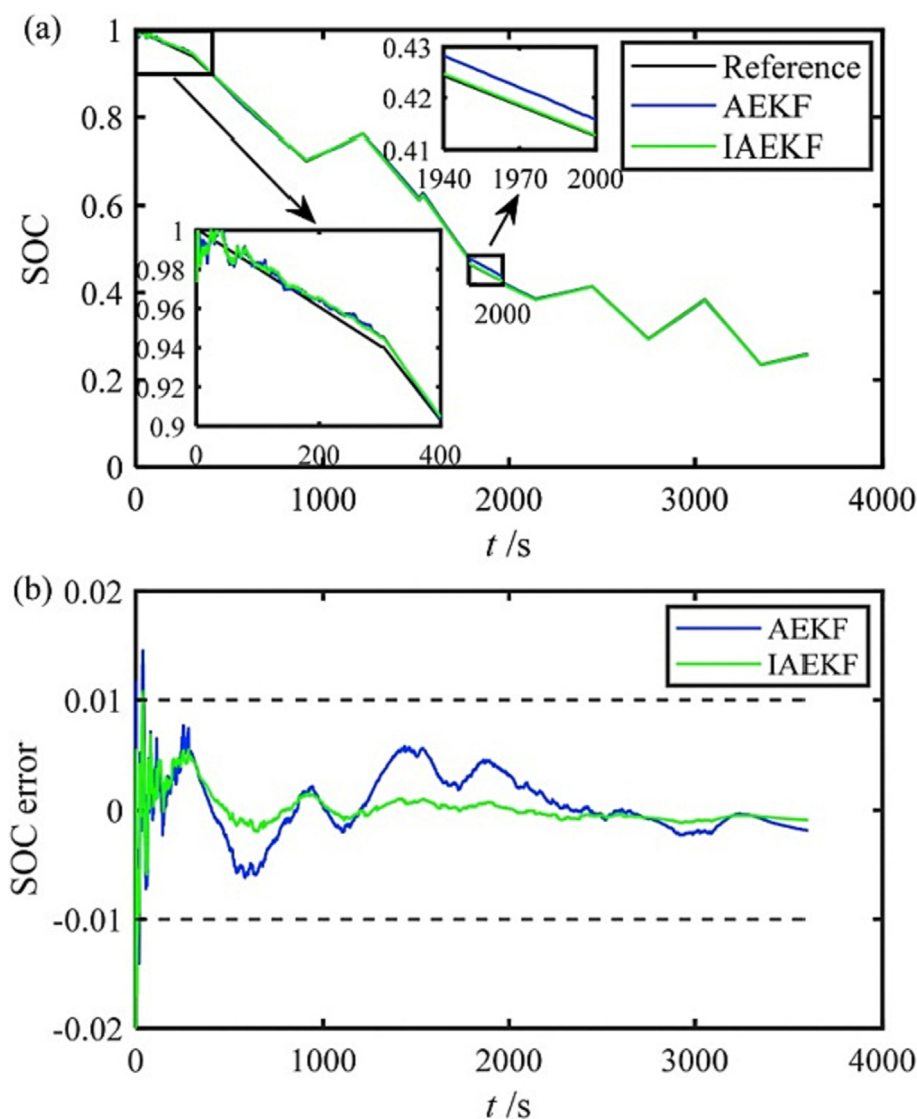

Fig. 3. Schematic diagrams of (a) Estimated SOC, (b) its error. Reproduced from Ref. [24] with permission from Elsevier.

data such as SOC and SOH predictions, it is possible to divide the data into n segments so that the algorithm does not struggle with fine-grained values, use One-hot encoding for classification, or define it as a time series problem, and finally combine the features to obtain the correlation. In their ground-breaking work, Severson et al. [39] predicted battery life and classified high and low life through high-correlation features generated from 124 battery data sets that reach 80% of rated capacity.

And, for ML, a thorough analysis of the data during the data preprocessing, and determining the impact of each variable on the results will help to further adjust the training data to achieve consistent trends and accurate predictions. The summary of recent works on ML methods for LIBs state predictions is listed in Table 3.

3.2. Deep learning

Although traditional ML methods can estimate the capacity with high accuracy, they have some limitations. They usually require complex feature engineering to achieve good performance, consistently include exploratory data analysis, reducing the data dimensions to facilitate processing, and selecting the best features for the ML algorithms. Inappropriate feature extraction may limit the performance of traditional ML, and it can be difficult to determine the appropriate features that represent the most useful information for capacity estimation.

As a subset of ML, DL uses neural networks with more complex structures and layers to complete classification or regression tasks. Compared to traditional ML techniques, DL, such as CNN, RNN, etc., can learn from raw input data and multi-dimensional mapping relationships without introducing hand-coded rules or expert knowledge [70–72]. The main differences between ML and DL in capacity estimation are summarized in Fig. 5.

Regarding the use of neural networks, the existing research can be classified into separate models and combination models. The former was created to solve time series problems, such as standard RNN, including related variants, LSTM, Bidirectional LSTM (Bi-LSTM), gated recurrent unit (GRU), etc. The other is to combine different models, aiming to synthesize the advantages of each model in LIBs time series processing to achieve the effect of synergy effects, such as using the CNN-LSTM architecture, which can simultaneously capture features that affect battery degradation and hide the advantages of time dependence in features. dependence in features [73].
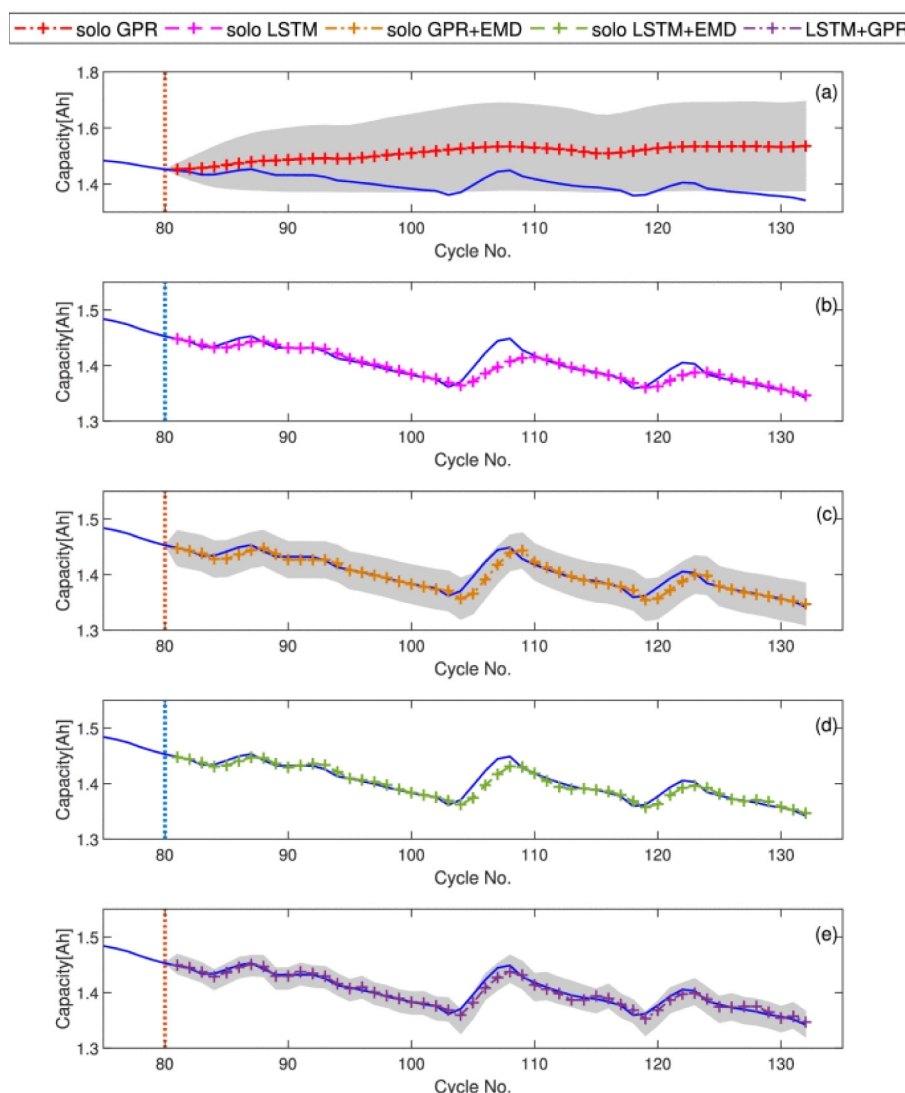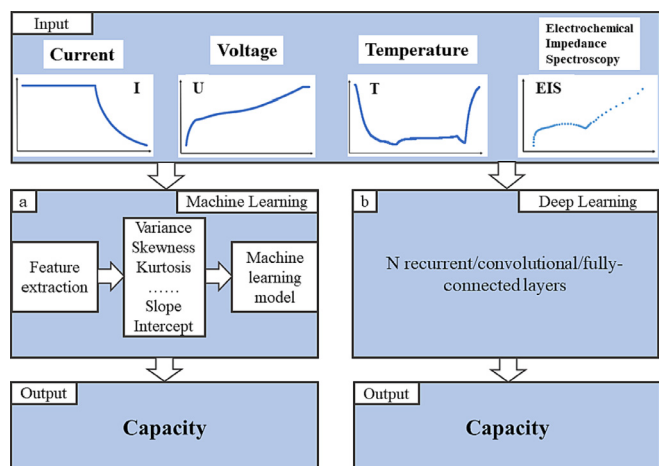

Fig. 4. Schematic diagrams of (a) GPM, (b) LSTM, (c) GPM + EMD, (d) LSTM + EMD, (e) LSTM + GPM. Reproduced from Ref. [41] with permission from IEEE.

Table 3
Summary of research in Battery state prediction using ML in the recent five years.

Ref	Data used							Algorithm			Prediction task			Error (%)	Dataset
	Current	Voltage	Capacity	Cycle number	EIS	Temperature	LR	GR	SVM	DT	SOC	SOH	RUL		Number of batteries
Zhang et al [36]					○			○					○	-	8
Nuhic et al [37]			○	○		○			○		○	○	○	-	6
Severson et al [39]	○	○	○	○			○						○	9.10	124
Liu et al [41]	○	○	○			○		○					○	4.20	7
Liu et al [55]		○	○				○					○		8.20	35
Yang et al [64]	○	○			○			○				○	○	<6.00	10
Patil et al [65]	○	○	○	○		○			○				○	7.87	19
Zhou et al [66]	○	○				○			○				○	5.90	3
Meng et al [67]	○	○				○			○			○		0.89	-
Zhu et al [68]			○		○	○				○			○	4.80	138
Zhang et al [69]	○	○								○		○		2.09	4

The circles in the table represent the data, algorithms and tasks used in the corresponding reference.

Fig. 5. The main differences between traditional ML and DL methods in the capacity estimation. (a) Traditional ML methods and (b) DL methods.

Deep Neural Network (DNN) is suitable for processing one-dimensional data [70], CNN can be better in processing multi-dimensional data [74], and RNN can process time series or related input data [41]. In addition, the layers and structure of CNN and RNN are much more complex than those of DNN. Therefore, CNN and RNN need more time to train the model, and DNN is more suitable for practical applications in most cases, but the neuron structure is relatively simple, and the upper limit may be lower.

3.2.1. Deep neural network

In DNN, the neural layers are divided into different layers according to the order of information received by each neuron. The inputs of neurons in each layer are the outputs of the neurons from the previous layer. The specific algorithm is shown in Eqs. (3) and (4).

$$Z^{(1)} = W^{(1)} \cdot a^{(1-1)} + b^{(1)} \tag{3}$$

$$a^{(1)} = f_1(Z^{(1)}) \tag{4}$$

In Eqs. (3) and (4), $Z^{(1)}$, $W^{(1)}$, $a^{(1)}$, $b^{(1)}$, and f_1 represents the input of layer l neurons, the weight matrix from the upper layer of layer l to layer l, the output of layer l neurons, the bias from the upper layer of layer l to layer l, and the activation function of layer l neurons respectively.

Khumprom et al. [70] predicted SOH and RUL of LIBs by DNN, and its effectiveness is verified by comparing to other ML algorithms. This work can be used as a benchmark reference for applying DL methods to general forecasting data. Chemali et al. [71] predicted the SOC by DNN through LIBs data of the vehicle driving cycle obtained at a variety of ambient temperatures. Most of the completed research is based on very uniform testing, so it is more convincing to use real-world data during dynamic operations for verification. Most of the data used in research on batteries RUL is limited to batteries cycle data in the laboratory. Modeling and forecasting using data with few influencing factors and a stable and unchanging environment usually have a high degree of accuracy. Compared with this kind of data, field data from practical applications show irregular circulation patterns, changing operating conditions, and path-dependent degradation mechanisms, making reliable predictions difficult. The accuracy of modeling and prediction using actual road condition data may not be as good as that obtained in the laboratory, but the robustness is better than it. And in order to prevent overfitting, the data augmentation method was used in this work to add the right amount of noise to enhance learning ability. Song et al. [72] proposed an intelligent SOH estimation framework using DNN, which can analyze the aging trend based on a data platform, and evaluate the residual capacity of the batteries. Roman et al. [75] proposed an ML pipeline that can estimate the cell SOH and algorithm uncertainty in real-time. It has no constrain on the battery type and operating conditions and can estimate the SOH at any time point in the battery life cycle within 15 minutes.

For the early life prediction problem, Tian et al. [76] developed an estimation for a full charging profile by taking a small subset of features of the charging profile as input, the charging curve can be accurately captured in less than 10 minutes and has the advantage of transfer learning (TL). Hsu et al. [77] developed a DNN with a novel architecture to predict RUL data for LIBs and achieved a
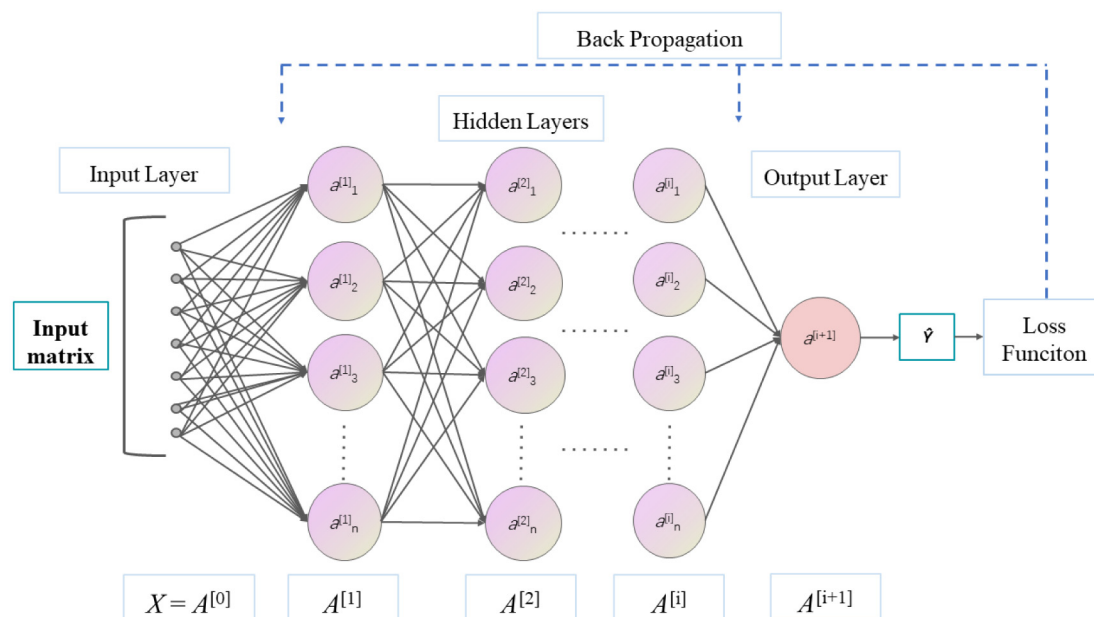
Fig. 6. Illustration of the DNN structure.

mean absolute percentage error of 6.46% using only one loop. They also used it to predict the cycle-by-cycle curve of used batteries for the first time. The DNN structure is illustrated in Fig. 6.

3.2.2. Convolutional neural network

CNN is a variant of neural networks with a convolution structure (convolution layer and pool sampling layer). It is composed of local receptive fields, shared weights sharing and pooling layers. Feature extraction is the characteristic of the algorithm [78]. The algorithm is shown in Eqs. (5) and (6).

$$Z^p = W^{p,d} \bigotimes X^d + b^p \tag{5}$$

$$Y^p = f(Z^p) \tag{6}$$

Where Z^p is the output sum of layer $1 \sim D$ neurons; $W^{p,d}$ is the weight matrix of layer d; X^d is the input of layer d neurons; b^p is the bias; and f is the activation function.

As a fitter for nonlinear dynamic systems, CNN can map a series of measurable parameters such as voltage, current, and capacity over a period to a target state. For SOH prediction, it is necessary to consider the difference in data characteristics of the same features in the local scope, which coincides with the characteristics of local links and weight sharing of CNN. For SOC prediction, usually a one-dimensional CNN (1DCNN), which has the advantages of processing one-dimensional signals and low computational complexity.

Traditional ML methods are limited to the lack of the ability to extract all due value from large amounts of data and their high reliance on the extracted features. Failure to identify suitable features can lead to poor predictive performance. To solve this issue, Shen et al. [74] proposed a capacity estimation method based on voltage, current, and charging capacity in the partial charging cycle using deep CNN. This method uses the local connectivity and shared weight of deep CNN for estimating the battery capacity by the measured values during charging, which produces a higher accuracy and robustness in the online estimation. Different types of

batteries, such as LiFePO₄ and lithium nickel cobalt manganese, have different charge–discharge performances and lifetimes, which may lead to changes in the shape of the charge–discharge curves. To reduce the influence of the random workload of the device on the prediction, Yang et al. [79] proposed a method based on the fusion of three-dimensional and two-dimensional CNN. The former CNN layer can fuse the V/I/T curve and the difference between periods by considering the relationship. The latter CNN layer can fully and automatically extract the information from these curves.

Almost all data-driven methods need much raw data, and some require large amounts of voltage, current, or temperature data acquired during charging or discharging to extract features such as maximum temperature and maximum voltage [65]. Others require voltage, current, temperature, or capacity data in cycles to achieve features such as kurtosis, skewness, and variance of discharge capacity or differences in discharge voltage curves [39]. However, data satisfied are usually acquired in the laboratory. In many situations, the random behavior of users leads to these two types of raw data being difficult to obtain. To cope with this problem, Qian et al. [80] proposed a method based on 1DCNN, which randomly selected a section of the charging curve as the input for capacity estimation. To improve the robustness and accuracy, the linear decreasing weighted particle swarm optimization algorithm has been demonstrated with the capability to find excellent hyperparameters, which is used to optimize the local super parameters of the neural networks.

In the process of obtaining experimental data, random errors in the measurement variables are inevitable. This kind of interference data will not only increase the amount of data, but also increase the amount of calculation, which in turn affects the convergence speed and accuracy, so it is of great significance to obtain a pure data set through denoising. Yang et al. [73] proposed a hybrid neural network combining CNN and Bi-LSTM, and used complete set empirical mode decomposition, independent component analysis, and interval thresholding for data denoising to help information learning to predict RUL of lithium-ion containers. Yang et al. [81]

handled partial discharge SOH between two consecutive charge/discharge cycles to cope with data truncation through CNN. Aiming at the large fluctuation of SOC and the accumulation of estimation errors in continuous time steps, Bian et al. [82] proposed a method that combines multichannel CNN and bidirectional RNN (MCNN-BRNN). Traditional CNN [83,84] does not treat measurement sequences as separate individuals and performs convolution on a single path, while MCNN can extract unaffected by perturbation and multi-scale locally robust features from different input paths, thereby reducing estimation fluctuations and enhancing the robustness of the estimator. Furthermore, global convolutional layers aim to the interrelationships of multi-scale features and maintain temporal coherence.

Collecting actual operating cycle data is a laborious and time-consuming process, how to solve the problem of insufficient data is crucial. Shen et al. [85] proposed a method combining TL and ensemble learning. Eight deep CNN sub-models were used for pre-training, and then shared the parameters to the target task. The obtained deep CNN-TL model was integrated to construct the deep CNN ensemble TL model. This method can ameliorate the accuracy of capacity estimation, and ensemble learning enhances the possibility of choosing an algorithm with an excellent performance by combining the prediction results of multiple learning algorithms, which can effectively improve the robustness of capacity estimation. Considering the relationship, the parameters from the pre-train model can be transferred through TL to speed up and optimize the learning efficiency of the model, make the process of training complex neural networks converge when relatively few training data are used in the target task, and ameliorate the performance by the knowledge learned from the source task. And to reduce the size and computational complexity of the model while maintaining the model performance, so the model can predict capacity online and fast. Li et al. [86] used a pruned CNN approach assisted with TL with a fine-tuning strategy to obtain the best accuracy and computational efficiency in comparison with conventional CNNs. In addition, two aspects of the accuracy and response speed of the system must be considered. For time series problems, RNN and its variants are popular in interpreting sequence inputs, but they are limited in capturing considerably long-term relationships. On the other hand, dilated CNN has proven its capability for capturing long-term relationships [87]. Therefore, Hong et al. [88] proposed a DL framework that from original data to prediction target, which seeks more discriminative decline characteristics by correlating the time series and cross data in the original data, with an average absolute error rate of 10.6%. This method not only predicts the RUL of LIBs in a short time (25X faster) but quantifies the uncertainty in neural network prediction.

3.2.3. Recurrent neural network

RNN is a kind of neural network with the ability of short-term memory. It is shown that a neuron can not only accept the input of other neurons, but also accept its own feedback [89]. The specific algorithm is shown in Eqs. (7) and (8).

$$Z_t = Uh_{t-1} + Wx_t + b \tag{7}$$

$$h_t = f(Z_t) \tag{8}$$

Where Z_t is the net input of the hidden layer; U is the state-to-state weight matrix; h_{t-1} is the state of the hidden layer from the upper layer of layer t to layer t; W is the state input weight matrix; x_t is the input value; b is the offset; and f is the activation function.

Compared to CNN, the main feature of RNN is that it has a memory function. This memory function refers to the fact that the current output of a sequence is not only related to the current input,

but also to the output of the previous sequence. The information is memorized and applied to the calculation of the current output.

Due to the inherent mechanism of RNN [90], it is prone to gradient disappearance in long-term sequence tasks, so it is impossible to capture the long-term dependence of data [91]. Introduce gating mechanisms to overcome this limitation, such as LSTM [92] and GRU [93] is the most effective approach. There are fewer GRU parameters, so it is easier to converge. Structurally, GRU has only two gates (update and reset), LSTM has three gates (forget, input, output), GRU directly passes the hidden state to the next unit, while LSTM uses a memory cell to wrap the hidden state.

RNN has strong adaptability to dynamic loading, Kwon et al. [94] used the voltage to predict the RUL of lithium nickel cobalt manganese oxide batteries and obtained 0.21% error within the 5% prediction interval Xi et al. [95] proposed a time-delayed RNN, which is more suitable for LIBs SOC state estimation and compared with the equivalent circuit model. For the long-range dependency problem in RNNs, Feng et al. [96] proposed the use of clockwork RNN for SOC estimation. Compared to RNN, the network divides the hidden layer into several independent modules, which can not only capture long-term relationships, but also could capture rapid changes, and assist to capture the internal characteristics of the LIBs better while reducing the computational cost.

Based on RNN, LSTM adds an input gate, forget gate, and output gate to learn long-term dependencies between data. Aiming at solving the problem that traditional LSTM lacks an effective ability to capture the large changes in local regions, Wang et al. [97] proposed a Local Tangent Space Alignment (LTSA) feature extraction and Adaptive Sliding Window (ASW) LSTM for RUL Prediction. health indicators are extracted from monitoring data by LTSA, while ASW LSTM is employed to learn long-term dependencies, capture local regeneration, and predict LIBs degradation trends. Wang et al. [98] proposed a method based on autoregressive integrated moving average, Bi-LSTM, and Bayesian Optimization (BO), which predicts the linear and nonlinear parts of the time series task separately, and then uses BO for tuning. Yang et al. [73] combined CNN and bidirectional Bi-LSTM for LIBs remaining lifetime prediction. Ren et al. [47] proposed a model to predict the RUL of LIBs by augmenting the raw data with an autoencoder, CNN mining battery depth information, and LSTM for time series prediction. Qu et al. [33] proposed a network that ensemble particle swarm optimization, attention mechanism, and LSTM. The method applies a fully integrated empirical mode decomposition with adaptive noise to the raw data and utilizes an attention mechanism to dynamically focus on certain parts of the data that help perform the task. Cicek et al. [99] developed a smartphone app using a CNN-LSTM network, demonstrating the potential of DL to predict the state of LIBs for a wide range of applications.

For the problem that data-driven methods require many training samples, Han et al. [100] proposed a novel LSTM framework assisted with domain adaptation, which building a general capacity estimation model for differential batteries that can be used with only a small amount of cycle data by capturing the nonlinear mapping of voltage and current to capacity by LSTM and integrating a domain adaptation layer into the LSTM for degenerate feature alignment. Heinrich et al. [101] presented a novel data-driven approach for battery SOH estimation based on the virtual execution of battery experiments. The LSTM model has been used to simulate the electric response during capacity testing, incremental capacity analysis, and peak-power testing by learning the electrical behavior of an automotive battery cell based on in-vehicle driving data. Ma et al. [102] proposed a hybrid TL scheme for RUL prediction of different battery formulations. Zhu et al. [103] used six

types of features extracted from voltage relaxation to estimate the capacity, and achieved 1.6% of RMSE using support vector regression and TL. Estimated results of one example of the capacity and error of LIBs by LSTM are shown in Fig. 7.

As mentioned earlier, LSTM was proposed in order to overcome the inability of RNN to handle long-distance dependencies. As a simplified form of LSTM, GRU maintains the effect of LSTM while making the structure simpler [104]. And in embedded implementations, GRU is more suitable than LSTM [105].

In order to describe the uncertainty of RUL prediction and avoid overfitting, Wei et al. [106] proposed a method that combines the Monte Carlo Dropout and GRU methods. Yang et al. [90] proposed a DL method based on a two-stage attention mechanism, which uses an attention mechanism in the encoder stage to extract useful information from the input sequence features, another attention mechanism is used in the decoder stage to consider the correlation of time series. Outperforming forecasting results come from suitable data. Only using temperature data, it would be great to extract the wealth of information on health features from temperature difference curves for SOH estimation [107]. Cui et al. [108] extracted six health features from the operational process and introduced dynamic spatiotemporal attention-based GRU for SOH estimation. With a small sample set, Che et al. [109] combined TL and GRU to estimate RUL from health features extracted from partial voltage profiles during fast-charging operations. In another example, [110] an improved SOC estimation method based on GRU and TL was proposed.

3.2.4. Brief summary

There are many factors that should be considered when choosing an appropriate ML method, such as the amount of data available, the quality of results required, the speed of operations asked, and the interpretability of models demanded.

Although the data generated by LIBs are plentiful, the available data is scarce, so researchers have turned their attention to TL, hoping to solve the problem of data scarcity. TL can learn a model for one task and then use it to solve other related tasks [111]. As a member of prognostics and health management, the SOH of LIBs is also highly time-dependent like the SOH of aviation equipment, electronic systems, robotic systems, etc., which means that the health status data obtained from other devices may also be applicable [112]. Due to the different formulation batteries, their charge–discharge curves and life-span curves are different. In addition to pre-train, a model can also be trained by fine-tuning and then used in a new task. It is fine-tuned to make the model better adapt to the new task to solve this problem [102,103].

In DL, the research of artificial intelligence (AI) lies in the optimization of both data and models. For the data part, the limitation is that the amount of valuable data is lacking. On the one hand, the data cycle is long, and the amount of available data is difficult to collect. On the other hand, the application environment and chemical composition are complex, and under the influence of multi-dimensional factors, it is difficult to analyze all aspects to obtain the most valuable features. Approaches such as data augmentation and TL can help to deal with this difficulty. For the model part, RNN has good performance on time series problems, but it also has the problem of not being able to handle long-distance dependencies, and the model complexity is also high, so LSTM and GRU were born [104]. Model complexity is always an important fundamental issue, which can be explained as expressive ability and effective model complexity. The complexity of the model not only affects the learnability of the model on specific problems and data, but also the generalization ability of unseen data. Within an appropriate range (computing resources), the larger the data scale and diversity, the richer the amount of information contained in the data, and the more beneficial to the research task. Like the size of the data, the more complex the model, the better the effect. A complex model can "think" problems from a higher-dimensional perspective, and even excess parameters can enhance the robustness of the model [113]. It is not only affected by the model architecture itself, but also by the data distribution, data complexity, and amount of information. It is generally believed that model framework, model size, optimization process, and data complexity are four important factors affecting model complexity [114]. The choice of model framework affects the complexity of the Tanh, ReLU), etc. The size of the deep model, such as the number of
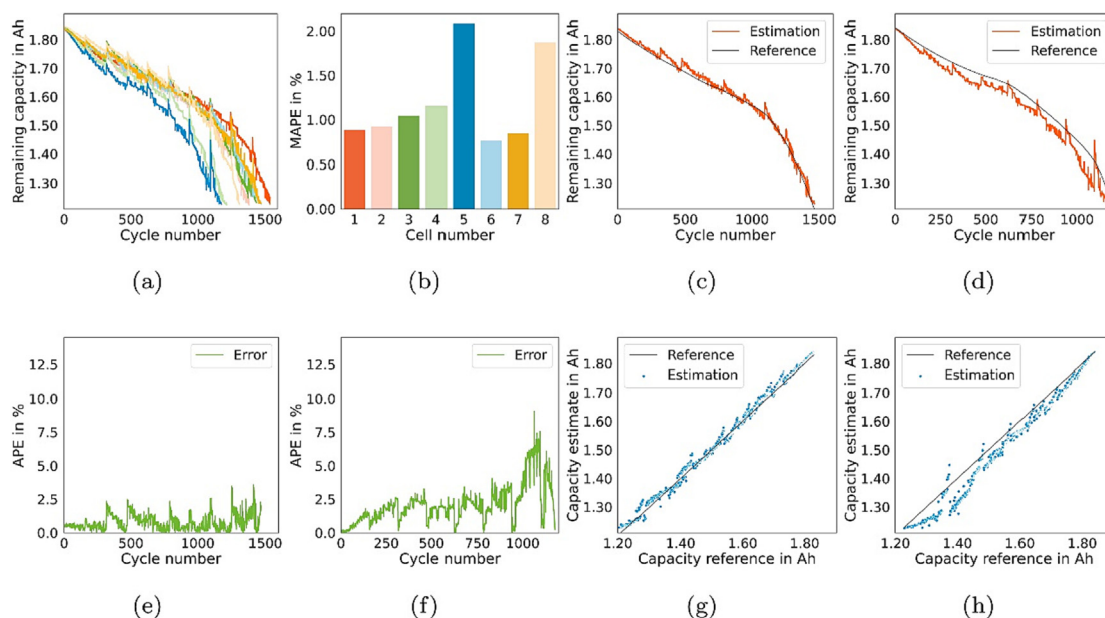

Fig. 7. Schematic diagrams of (a) estimated maximum capacity vs. cycle number plot for all 8 cells, (b) MAPE comparison of all 8 cells, (c) best-case cell, (d) worst-case cell, (e) best-case cell, (f) worst-case cell, (g) best-case cell, (h) worst-case cell, over their lifetime. Reproduced from Ref. [139] with permission from Elsevier.

parameters, the number, and width of hidden layers, the number, and size of filters, etc. will affect the complexity of the model. The optimization process affects the complexity of the model, including the form of the objective function, the choice of learning algorithm, and the setting of hyperparameters. The data on which the model is trained also affects the complexity of the model. The main influencing factors include data dimension, data type, and data type distribution. One example reduces the model size and computational cost by pruning [86].

Most ML algorithms have hyperparameters, which can be used to adjust the training process of the entire network, such as the number of hidden layers and complexity of the structure of the neural network, and so on. Hyperparameters are not directly involved in the training process, during the training process, only the parameters are updated, so it is necessary to optimize the hyperparameters, which can train a more efficient ML model more scientifically. The mainstream hyperparameter tuning techniques are grid search, random search, and Bayesian search.

In traditional tuning, it is most common to train the algorithm by randomly tuning manually and choosing the most suitable set of parameters. As a trial-and-error method, this method relies on experience, does not guarantee the best combination of parameters, and consumes more time.

Grid search is a basic hyperparameter tuning technique. It can evaluate and select the best model, but it takes a long time. Yao et al. [115] proposed a grid search method to optimize kernel function parameters and penalty factors, which can guarantee the accuracy and robustness of SVM. In many cases, all hyperparameters may not be equally important, and random search can replace grid search with better results but is not guaranteed to get the best combination of parameters.

BO is used by many researchers to adjust the hyperparameters of neural networks [116,117]. Its biggest advantage is sample efficiency, that is, BO can find a better combination of hyperparameters with very few steps. This optimization method has been used in some examples [98,118].

Compared to other ML methods, neural networks have high accuracy, so it is probably the most widely used method for prediction, not only in the LIBs field, but also in supercapacitors [119]. During the charging and discharging of batteries, much experimental data is generated in each cycle. Almost all experimental data can be used to estimate the SOC of LIBs. This feature makes the neural network perform well in estimating the SOC. However, the data required to predict SOH or RUL is usually retrieved only once in each cycle, resulting in a sharp decrease in the amount of data available. In this case, the selected ML method needs to take more account of the impact of the amount of data on the results. In the absence of data, the accuracy of DL cannot be guaranteed. For example, if there is a relative lack of data, GPM may be a better choice. More importantly, because the GPM inherently predicts uncertainty and its capability of capturing nonlinear relationships between features, it can be used for the SOH diagnosis of batteries [120]. If RUL is expressed by cycle numbers, then random forests may be a more appropriate method. In addition, since many ML methods are black-box models, LR may be preferred when considering security and strong explanations. In addition, the data selected should be adjusted according to the purpose of the study. In term of accuracy, the battery data with static charge and discharge curves are used to estimate SOH with high accuracy. For validation of the robustness and reliability of the model, the battery data with cyclic dynamic curves can be used to validate the robustness and reliability of the approach. The summary of recent five years of work on DL methods for LIBs state predictions and the

advantages and disadvantages of the data-driven are shown in Tables 4 and 5 respectively.

4. Conclusions and perspectives

4.1. Conclusions

LIBs can be widely used in a variety of scenarios through their high energy and power density and have become one of the indispensable key devices in modern life [121]. However, the key limiting factor in advancing these technologies is the unpredictability of battery degradation. Only by accurately predicting SOH and RUL can the user be notified in time that the battery should be replaced to avoid accidental capacity degradation and accidents such as battery explosion [122]. In addition, battery prognosis is critical to determining whether the battery can be recycled as scrap metal or used in less demanding "second-life" applications [123].

The training of model-based methods is very simple, but the complexity of the model varies. Recently, the popular data-driven method has the good nonlinear fitting ability, but the complexity is higher than the statistical method. Although there have been many studies on battery RUL prediction, more progress is needed in this area. The main challenge is related to the practicality and applicability of the RUL prediction method in applications.

4.2. Perspectives

RUL prediction of LIBs is a promising but challenging task. Despite the rapid development in recent years, the field is still in its early stage, and current research is mainly focused on model-based and data-driven approaches.

The data-driven approach realized by AI has been developed rapidly in the past ten years because of its huge potential [124]. At the same time, it has also opened a new research way to experimental subjects such as batteries. Through continuous learning and optimization, based on a large amount of data, predicting by AI is efficient, accurate, and robust. There are many models with powerful performance, which can be used in various applications if there is a lot of corresponding data. Many batteries equipment operates every day in the world, but it is difficult to obtain data, and the data is only in the hands of battery companies, making it impossible for many researchers to carry out experiments. The existing public battery data sets are provided by the Prognostics Center of Excellence at NASA Ames [125], the Center for Advanced Life Cycle Engineering at the University of Maryland [126,127], and Severson et al. [39].

The amount of data is not enough for AI, especially for DL, and the shape of the battery, the positive electrode, the negative electrode, the electrolyte, and working conditions are also diverse. In this case, TL is used for pre-train. Considering the correlation between prognostics and health management fields, the parameters can be shared with the new model through TL. In addition, in order to take advantage of the scarce data and avoid fitting some unimportant features, adding artificially designed prior information to the model can allow the model to learn some key characteristics. Finally, a hybrid approach by combining knowledge-driven and data-driven approaches and making good use of their respective advantages is competitive. Unlike the way computer learns through a large amount of data and time, the knowledge-driven method does not require a long learning process and can respond quickly. By constructing knowledge-driven and data-driven hybrid models, they can complement each other to prevent error accumu-

Table 4
Summary of research in Battery state prediction using DL in the recent five years.

Ref	Data used						Algorithm		Prediction task				Dataset	Number of batteries
---	Current	Voltage	Capacity	Cycle number	EIS	Temperature	DNN	CNN	RNN	SOC	SOH	RUL	Error (%)	
Qu et al. [33]	○	○	○						○		○	○	-	3
Nikolian et al. [47]		○	○			○		○	○			○	5.03	18
Khumprom et al. [70]	○	○			○		○				○	○	3.42	4
Chemali et al. [71]	○	○				○	○			○			1.10	-
Song et al. [72]	○	○	○				○				○		4.50	700
Roman et al. [75]	○	○	○			○	○				○		0.45	179
Hsu et al. [77]	○	○	○			○	○					○	6.46	158
Shen et al. [78]	○	○						○		○			0.88	28
Yang et al. [79]	○	○				○		○				○	3.6	124
Qian et al. [80]	○	○	○					○			○		4.2	8
Bian et al. [82]	○	○				○		○	○	○			1.01	-
Shen et al. [85]	○	○						○			○		1.90	28
Li et al. [86]	○	○	○					○			○		0.83	20
Hong et al. [88]	○	○				○		○				○	10.60	124
Kwon et al. [94]					○				○			○	1.43	-
Xi et al. [95]	○	○							○	○			2.5	-
Feng et al. [96]	○	○				○			○	○			1.29	-
Wei et al. [107]	○	○							○			○	1.00	4
Chen et al. [108]	○	○				○			○		○		2.28	8
Che et al. [110]		○							○		○	○	2.00	124

The circles in the table represent the data, algorithms and tasks used in the corresponding reference.

Table 5
Comparison of different data-driven methods.

Property	LR	GPM	SVM	DT	DNN	CNN	RNN
Advantage	• Easy to understand, the results are interpretable	• Handling high-dimension and small size datasets	• Capable of dealing with the local minimum, nonlinear, and small sample size problems	• Easy to understand and explain Simple data processing	• High accuracy High learning capability	• Weight sharing strategy reduces training parameters Pooling operation reduces the spatial resolution	• Model time series content.
Disadvantage	• Difficult to model nonlinear data and express highly complex data	• High computational load with large datasets Lack of sparseness	• Kernel functions need to satisfy the mercer criterion	• Sample size is critical Easy to overfit	• Study time is too long The results are difficult to explain	• Deep models are prone to vanishing gradient problems	• Prone to gradient dissipation or gradient explosion problems

lation and unexpected changes (such as battery safety status warnings).

Metal ion batteries, solar cells, and fuel cells have the complex characteristics of a battery reaction system [128-130]. The models and methods in LIBs are also useful for the other systems. At present, many battery mechanism explanations have been recognized, but there are still unclear areas. The complexity, non-linearity and priori knowledge of DL technology determine that the combination with the battery field will certainly make great progress in battery research. In the future, DL in the batteries field will burst with more power not only by the latest technologies, such as Transformer, graph neural network, pre-train model, and temporal CNN, but by combining the estimation of battery status with electrochemical models and prediction of new materials with high-throughput calculations, phase-field method, and quantum chemistry [131–133] (Fig. 8).

4.2.1. Combining electrochemical models with machine learning approaches

Because external factors such as temperature, operating conditions, and charging–discharging conditions are not controllable, the model-based decay process is not comprehensive enough.

Many researchers have studied the traditional electrochemical model deeply and extensively [31–33]. The explanation of its reaction mechanism is more complete, but there is still some knowledge outside the field of human knowledge. Furthermore, the current electrochemical models are more specific, each model can well represent a specific reaction mechanism, but it also leads to the problem of weak generalization performance. These two examples demonstrate the feasibility of combining electrochemical models and ML [134,135].

In addition, in terms of parameter settings, the traditional model-based method sets the initial parameters randomly or relies on experience, which is time-consuming and labor-intensive. By combining with genetic algorithms, it is possible to obtain better optimization results with a faster convergence speed when solving more complex combinatorial optimization problems. In the process of battery use, the battery is constantly degrading, and the parameters need to be updated to maintain prediction accuracy. This situation can be completed by filtering algorithms.

4.2.2. Using computer vision and atomic simulation technology

Combined with computer vision technology in ML, in terms of material performance testing, materials morphology can be used
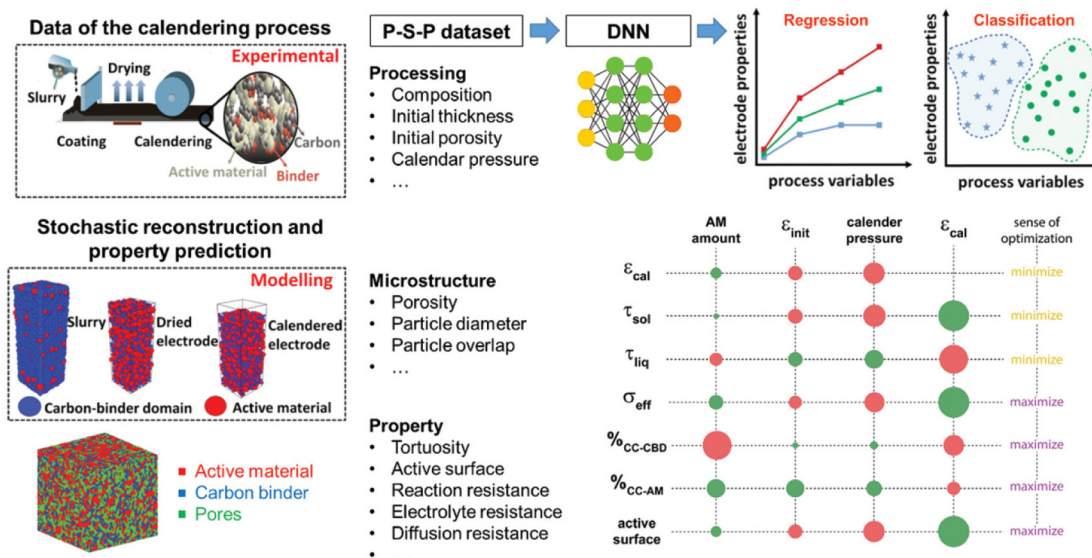
Fig. 8. Schematic diagrams of ML framework for the design of processing parameters and microstructure features. Reproduced from Ref. [140] and Ref. [141] with permission from Wiley and Elsevier.

to judge such issues as lithium dendrite growth, SEI film growth, cracking degree, dissolution of active substances, structure collapse state, and so on [136,137]. Those can be associated with SOC and SOH to achieve more accurate predictions. Finally, based on ML, using accurate potential energy surfaces and complex numerical data, the energy can be quickly estimated, especially at the power-on interface, which can adjust the Fermi level of the material, thus realizing the regulation of the electronic energy [138].

With the growing scale of battery usage, the accurate estimation and prediction of battery status will obtain much attention in the future. This article mainly provides a comprehensive understanding of the SOH and RUL of LIBs predicted by AI, and provides a perspective for the development of prediction algorithms, hoping to promote the rapid development of LIBs as safe, reliable, and efficient energy storage devices.

Declaration of competing interest

The authors declare that they have no known competing financial interests or personal relationships that could have appeared to influence the work reported in this paper.

Acknowledgments

References

[1] R. Schmuch, R. Wagner, G. Hörpel, T. Placke, M. Winter, Nat. Energy. 3 (2018) 267–278.
[2] Y. Zheng, Z. Shi, D. Ren, J. Chen, X. Liu, X. Feng, L. Wang, X. Han, L. Lu, X. He, M. Ouyang, J. Energy Chem. 69 (2022) 593–600.
[3] M. Broussely, P.h. Biensan, F. Bonhomme, P.h. Blanchard, S. Herreyre, K. Nechev, R.J. Staniewicz, J. Power Sources. 146 (2005) 90–96.
[4] J. Hu, F. Fan, Q. Zhang, S. Zhong, Q. Ma, J. Energy Chem. 67 (2022) 604–612.
[5] J. Liu, Z. Wang, J. Bai, J. Energy Chem. 70 (2022) 531–541.
[6] M. Ge, Y. Liu, X. Jiang, J. Liu, Measurement 174 (2021) 109057.
[7] K. Ando, T. Matsuda, D. Imamura, J. Energy Chem. 53 (2021) 285–289.
[8] C.Y. Wang, G.S. Zhang, S.H. Ge, T. Xu, Y. Ji, X.G. Yang, Y.J. Leng, Nature. 29 (2016) 515–518.
[9] L. Liu, X. Feng, C. Rahe, W. Li, L. Lu, X. He, D.U. Sauer, M. Ouyang, J. Energy Chem. 61 (2021) 269–280.
[10] J. Ding, R. Xu, C. Yan, B. Li, H. Yuan, J. Huang, J. Energy Chem. 59 (2021) 306–319.
[11] G.J. Offer, V. Yufit, D.A. Howey, B. Wu, N.P. Brandon, J. Power Sources. 206 (2012) 383–392.
[12] H. Tian, P. Qin, K. Li, Z. Zhao, J. Clean. Prod. 261 (2020) 120813.
[13] W. Li, M. Rentemeister, J. Badeda, D. Jöst, D. Schulte, D.U. Sauer, J. Energy Storage. 30 (2020) 101557.
[14] S. Wang, S. Jin, D. Deng, C. Fernandez, Front Mech. Eng. 7 (2021) 719718.
[15] S.M. Rezvanizaniani, Z. Liu, Y. Chen, J. Lee, J. Power Sources. 256 (2014) 110–124.
[16] W. Waag, C. Fleischer, D.U. Sauer, J. Power Sources. 258 (2014) 321–339.
[17] E. Wood, M. Alexander, T.H. Bradley, J. Power Sources. 196 (2011) 5147–5154.
[18] B. Lunz, Z. Yan, J.B. Gerschler, D.U. Sauer, Energy Policy. 46 (2012) 511–519.
[19] J. Neubauer, A. Pesaran, J. Power Sources. 196 (2011) 10351–10358.
[20] S. Zhang, X. Guo, X. Dou, X. Zhang, Sustain. Energy Techn. 40 (2020) 100752.
[21] Y. Zheng, M. Ouyang, X. Han, L. Lu, J. Li, J. Power Sources. 377 (2017) 161–188.
[22] M. Petzl, M.A. Danzer, IEEE T. Energy Conver. 28 (2013) 675–681.
[23] Q. Yu, C. Wan, J. Li, L., E,, X., Zhang,, Y., Huang,, T., Liu,, Energies. 14 (2021) 1797.
[24] D. Sun, X. Yu, C. Wang, C. Zhang, R. Huang, Q. Zhou, T. Amietszajew, R. Bhagat, Energy. 214 (2021) 119025.
[25] J. Meng, G. Luo, F. Gao, IEEE T. Power Electron. 31 (2016) 2226–2238.
[26] M.H.S. Segler, M. Preuss, M.P. Waller, Nature. 555 (2018) 604–610.
[27] H. Xu, J. Ma, P. Tan, B. Chen, Z. Wu, Y. Wu, H. Wu, J. Wang, M.N. Xuan, Energy and AI. 1 (2020) 100003.
[28] T. Hengl, M.A.E. Miller, J. Križan, K.D. Shepherd, A. Sila, M. Kilibarda, O. Antonijević, L. Glušica, A. Dobermann, S.M. Haefele, S.P. McGrath, G.E. Acquah, J. Collinson, L. Parente, M. Sheykhmousa, K. Saito, J.M. Johnson, J. Chamberlin, F.B.T. Silatsa, M. Yemefack, J. Wendt, R.A. MacMillan, I. Wheeler, J. Crouch, Sci. Rep. 11 (2021) 6130.
[29] M. Roberts, D. Driggs, M. Thorpe, J. Gilbey, M. Yeung, S. Ursprung, A.I. Aviles-Rivero, C. Etmann, C. McCague, L. Beer, J.R. Weir-McCall, Z. Teng, E. Gkrania-Klotsas, A. Ruggiero, A. Korhonen, E. Jefferson, E. Ako, G. Langs, G. Gozaliasl, G. Yang, H. Prosch, J. Preller, J. Stanczuk, J. Tang, J. Hofmanninger, J. Babar, L.E. Sánchez, M. Thillai, P.M. Gonzalez, P. Teare, X. Zhu, M. Patel, C. Cafolla, H. Azadbakht, J. Jacob, J. Lowe, K. Zhang, K. Bradley, M. Wassin, M. Holzer, K. Ji, M.D. Ortet, T. Ai, N. Walton, P. Lio, S. Stranks, T. Shadbahr, W. Lin, Y. Zha, Z. Niu, J.H.F. Rudd, E. Sala, C.B. Schönlieb, C. Aix, Nat. Mach. Intell. 3 (2021) 199–217.

[30] M.S. Ardejani, L. Noodleman, E.T. Powers, J.W. Kelly, Nat. Chem. 13 (2021) 480–487.
[31] M. Charkhgard, M. Farrokhi, IEEE T. Ind Electron. 57 (2010) 4178–4187.
[32] C.C. Liu, T. Wu, C. He, Adv. Mech. Eng. 12 (2020) 1–11.
[33] J. Qu, F. Liu, Y. Ma, J. Fan, IEEE Access. 7 (2019) 87178–87191.
[34] S.S.Y. Ng, Y. Xing, K.L. Tsui, Appl. Energy. 118 (2014) 114–123.
[35] K. Park, Y. Choi, W.J. Choi, H.Y. Ryu, H. Kim, IEEE Access. 8 (2020) 20786–20798.
[36] Y. Zhang, Q. Tang, Y. Zhang, J. Wang, U. Stimming, A.A. Lee, Nat Commun. 11 (2020) 1706.
[37] A. Nuhic, T. Terzimehic, T. Soczka-Guth, M. Buchholz, K. Dietmayer, J. Power Sources. 239 (2013) 680–688.
[38] Y. Liu, G. Zhao, X. Peng, IEEE Access. 7 (2019) 155130–155142.
[39] K.A. Severson, P.M. Attia, N. Jin, N. Perkins, B. Jiang, Z. Yang, M.H. Chen, M. Aykol, P.K. Herring, D. Fraggedakis, M.Z. Bazant, S.J. Harris, W.C. Chueh, R.D. Braatz, Nat Energy. 4 (2019) 383–391.
[40] L. Ren, J. Dong, X. Wang, Z. Meng, L. Zhao, M.J. Deen, I.E.E.E.T. Ind, Inform. 17 (2021) 3478–3487.
[41] K. Liu, Y. Shang, Q. Ouyang, W.D. Widanage, I.E.E.E.T. Ind, Electron. 68 (2021) 3170–3180.
[42] X. Hu, S.E. Li, Y. Yang, I.E.E.E.T. Transp, Electron. 2 (2016) 140–149.
[43] M.F. Ng, J. Zhao, Q. Yan, G.J. Conduit, Z.W. Seh, Nat. Mach. Intell. 2 (2020) 161–170.
[44] S.K. Rechkemmer, X. Zang, W. Zhang, O. Sawodny, J. Energy Storage. 21 (2019) 773–786.
[45] W. Zhang, D. Wang, W. Zheng, J. Energy Chem. 41 (2020) 100–106.
[46] W. Zhang, F. Ma, S. Guo, X. Chen, Z. Zeng, Q. Wu, S. Li, S. Cheng, J. Xie, J. Energy Chem. 66 (2022) 440–447.
[47] A. Nikolian, J. Jaguemont, J.D. Hoog, S. Goutam, N. Omar, V. Peter, J.V. Mierlo, I., J. Int. J. Elec. Power. 98 (2018) 133–146.
[48] N. Tian, Y. Wang, J. Chen, H. Fang, J. Energy Storage. 29 (2020) 101282.
[49] P. Nelson, D. Dees, K. Amine, G. Henriksen, J. Power Sources. 110 (2002) 349–356.
[50] D.G. Moye, P.L. Moss, X.J. Chen, W.J. Cao, S.Y. Foo, J. Power Sources. 435 (2019) 226694.
[51] T. Huria, G. Ludovici, G. Lutzemberger, J. Power Sources. 249 (2014) 92–102.
[52] J. Zhou, D. Liu, Y. Peng, X. Peng, I.E.E.E. Instrum, Meas. Mag. (2012) 2196–2199.
[53] Y. Zheng, Y. Cui, X. Han, M. Ouyang, Energy. 237 (2021) 121556.
[54] W. Yang, H. Xu, L. Chen, S. Hu, Stat. Pap. 59 (2018) 449–465.
[55] X. Liu, X. Zhang, X. Chen, G. Zhu, C. Yan, J. Huang, H. Peng, J. Energy Chem. 68 (2022) 548–555.
[56] D. Liu, J. Pang, J. Zhou, Y. Peng, M. Pecht, Microelectron. Reliab. 53 (2013) 832–839.
[57] J. Wang, Z. Deng, T. Yu, A. Yoshida, L. Xu, G. Guan, A. Abudula, J. Energy Storage. 51 (2022) 104512.
[58] N. Akhtar, X. Sun, M. Yasir Akram, F. Zaman, W. Wang, A. Wang, L. Chen, H. Zhang, Y. Guan, Y. Huang, J. Energy Chem. 52 (2021) 310–317.
[59] P. Dong, X. Zhang, K.S. Han, Y. Cha, M. Song, J. Energy Chem. 70 (2022) 363–372.
[60] L. Xu, Y. Yang, Y. Xiao, W. Cai, Y. Yao, X. Chen, C. Yan, H. Yuan, J. Huang, J. Energy Chem. 67 (2022) 255–262.
[61] X. Liu, X. Qian, W. Tang, H. Luo, Y. Zhao, R. Tan, M. Qiao, X. Gao, Y. Hua, H. Wang, S. Zhao, C. Lai, M. Titirici, N.P. Brandon, S. Yang, B. Wu, J. Energy Chem. 52 (2021) 385–392.
[62] G. Seo, J. Ha, M. Kim, J. Park, J. Lee, E. Park, S. Bong, K. Lee, S.J. Kwon, S.-P. Moon, J. Choi, J. Lee, J. Energy Chem. 67 (2022) 663–671.
[63] G. Ye, M. Zhao, L. Hou, W. Chen, X. Zhang, B. Li, J. Huang, J. Energy Chem. 66 (2022) 24–29.
[64] D. Yang, Y. Wang, R. Pan, R. Chen, Z. Chen, Energy Procedia. 105 (2017) 2059–2064.
[65] M.A. Patil, P. Tagade, K.S. Hariharan, S.M. Kolake, T. Song, T. Yeo, S. Doo, Appl. Energy. 159 (2015) 285–297.
[66] X. Zhou, S.J. Hsieh, B. Peng, D. Hsieh, Microelectron. Reliab. 79 (2017) 48–58.
[67] J. Meng, L. Cai, G. Luo, D.I. Stroe, R. Teodorescu, Microelectron Reliab. 88–90 (2018) 1216–1220.
[68] S. Zhu, N. Zhao, J. Sha, J. Energy Storage. 1 (2019) e98.
[69] Z. Zhang, L. Li, X. Li, Y. Hu, K. Huang, B. Xue, Y. Wang, Y. Yu, Int. J. Energy Res. 46 (2022) 1756–1765.
[70] P. Khumprom, N. Yodo, Energies. 12 (2019) 660.
[71] E. Chemali, P.J. Kollmeyer, M. Preindl, A. Emadi, J. Power Sources. 400 (2018) 242–255.
[72] L. Song, K. Zhang, T. Liang, X. Han, Y. Zhang, J. Energy Storage. 32 (2020) 101836.
[73] H. Yang, P. Wang, Y. An, C. Shi, X. Sun, K. Wang, X. Zhang, T. Wei, Y. Ma, eTransportation. 5 (2020) 100078.
[74] S. Shen, M. Sadoughi, X. Chen, M. Hong, C. Hu, J. Energy Storage. 25 (2019) 100817.
[75] D. Roman, S. Saxena, V. Robu, M. Pecht, D. Flynn, Nat. Mach. Intell. 3 (2021) 447–456.
[76] J. Tian, R. Xiong, W. Shen, J. Lu, X. Yang, Joule. 5 (2021) 1521–1534.
[77] C. Hsu, R. Xiong, N. Chen, J. Li, N. Tsou, Appl. Energy. 306 (2022) 118134.
[78] T.Y. Kim, S.B. Cho, Energy. 182 (2019) 72–81.
[79] Y. Yang, Appl. Energy. 292 (2021) 116897.
[80] C. Qian, B. Xu, L. Chang, B. Sun, Q. Feng, D. Yang, Y. Ren, Z. Wang, Energy. 227 (2021) 120333.
[81] N. Yang, Z. Song, H. Hofmann, J. Sun, J. Energy Storage. 48 (2022) 103857.
[82] C. Bian, S. Yang, J. Liu, E. Zio, Appl. Soft Comput. 116 (2022) 108401.
[83] Z. Huang, F. Yang, F. Xu, X. Song, K. Tsui, IEEE Access. 7 (2019) 93139–93149.
[84] X. Song, F. Yang, D. Wang, K.L. Tsui, IEEE Access. 7 (2019) 88894–88902.
[85] S. Shen, M. Sadoughi, M. Li, Z. Wang, C. Hu, Appl. Energy. 260 (2020) 114296.
[86] Y. Li, K. Li, X. Liu, Y. Wang, L. Zhang, Appl. Energy. 285 (2021) 116410.
[87] A. oord, S. Dieleman, H. Zen, K. Simonyan, O. Vinyals, Graves, A., Kalchbrenner, N., Senior, A., Kavukcuoglu, K., arXiv preprint. 125 (2016) 2.
[88] J. Hong, D. Lee, E.R. Jeong, Y. Yi, Appl. Energy. 278 (2020) 115646.
[89] A. Eddahech, O. Briat, N. Bertrand, J.Y. Délétage, J.M. Vinassa, Int. J. Elec. Power. 42 (2012) 487–494.
[90] K. Yang, Y. Tang, S. Zhang, Z. Zhang, Energy. 244 (2022) 123233.
[91] Y. Bengio, P. Simard, P. Frasconi, IEEE T. Neural Network. 5 (1994) 157–166.
[92] S. Hochreiter, J. Schmidhuber, Neural Comput. 9 (1997) 1735–1780.
[93] F. Yang, W. Li, C. Li, Q. Miao, Energy. 175 (2019) 66–75.
[94] S. Kwon, D. Han, J.H. Choi, J. Lim, S. Lee, J. Kim, J. Electroanal. Chem. 858 (2020) 113729.
[95] Z. Xi, R. Wang, Y. Fu, C. Mi, Appl. Energy. 305 (2022) 117962.
[96] X. Feng, J. Chen, Z. Zhang, S. Miao, Q. Zhu, Energy. 236 (2021) 121360.
[97] Z. Wang, N. Liu, Y. Guo, Neurocomputing. 466 (2021) 178–189.
[98] Z. Wang, J. Qu, X. Fang, H. Li, T. Zhong, H. Ren, Neurocomputing. 403 (2020) 63–79.
[99] E. Çiçek, S. Gören, Neural Comput. Appl. 33 (2021) 8017–8029.
[100] T. Han, Z. Wang, H. Meng, J. Power Sources. 520 (2022) 230823.
[101] F. Heinrich, M. Pruckner, J. Energy Storage. 48 (2022) 103856.
[102] J. Ma, P. Shang, X. Zou, N. Ma, Y. Ding, J. Sun, Y. Cheng, L. Tao, C. Lu, Y. Su, J. Chong, H. Jin, Y. Lin, Appl. Energy. 282 (2021) 116167.
[103] J. Zhu, Y. Wang, Y. Huang, R.B. Gopaluni, Y. Cao, M. Heere, M.J. Mühlbauer, L. Mereacre, H. Dai, X. Liu, A. Senyshyn, X. Wei, M. Knapp, H. Ehrenberg, Nat. Mach. Intell. 13 (2022) 2261.
[104] H. Zhang, J. Li, Y. Ji, H. Yue, I.E.E.E.T. Ind, Inform. 13 (2017) 616–624.
[105] L. Ungurean, M.V. Micea, G. Cârstoiu, Int. J. Energy Res. 44 (2020) 6767–6777.
[106] M. Wei, H. Gu, M. Ye, Q. Wang, X. Xu, C. Wu, Energy Reports. 7 (2021) 2862–2871.
[107] Z. Chen, H. Zhao, Y. Zhang, S. Shen, J. Shen, Y. Liu, J. Power Sources. 521 (2022) 230892.
[108] S. Cui, I. Joe, IEEE Access. 9 (2021) 27374–27388.
[109] Y. Che, Z. Deng, X. Lin, L. Hu, X. Hu, I.E.E.E.T. Veh, Technol. 70 (2021) 1269–1277.
[110] Y. Wang, Z. Chen, W. Zhang, Energy. 244 (2022) 123178.
[111] S.J. Pan, Q. Yang, I.E.E.E.T. Knowl, Data En. 22 (2010) 1345–1359.
[112] F. Yang, W. Zhang, L. Tao, J. Ma, Appl. Sciences. 10 (2020) 2361.
[113] B. Sébastien, S. Mark, 35th Conference on Neural Information Processing Systems. 34 (2021).
[114] X. Hu, L. Chu, J. Pei, W. Liu, J. Bian, Knowl. Inf. Syst. 63 (2021) 2585–2619.
[115] L. Yao, Z. Fang, Y. Xiao, J. Hou, Z. Fu, Energy. 214 (2021) 118866.
[116] S. Shin, Y. Lee, M. Kim, J. Park, S. Lee, K. Min, Eng. Appl. Artif. Intel. 94 (2020) 103761.
[117] J. Wu, X. Chen, H. Zhang, L. Xiong, H. Lei, S. Deng, J. Electron. Sci. Technol. 17 (2019) 26–40.
[118] M. Kim, H. Chun, J. Kim, K. Kim, J. Yu, T. Kim, S. Han, Appl. Energy. 254 (2019) 113644.
[119] J. Ren, X. Lin, J. Liu, T. Han, Z. Wang, H. Zhang, J. Li, Mater. Today Energy. 18 (2020) 100537.
[120] J. Ren, J. Cai, J. Li, Sci. Rep. 11 (2021) 12112.
[121] L. Zhang, C. Zhu, S. Yu, D. Ge, H. Zhou, J. Energy Chem. 66 (2022) 260–294.
[122] M. Long, T. Wang, P. Duan, Y. Gao, X. Wang, G. Wu, Y.-Z. Wang, J. Energy Chem. 65 (2022) 9–18.
[123] Y. Wang, N. An, L. Wen, L. Wang, X. Jiang, F. Hou, Y. Yin, J. Liang, J. Energy Chem. 55 (2021) 391–419.
[124] M. Haenlein, A. Kaplan, Calif Manage. Rev. 61 (2019) 5–14.
[125] B. Saha, K. Goebel, NASA AMES prognostics data repository, (2007).
[126] W. He, N. Williard, M. Osterman, M. Pecht, J. Power Sources 196 (2011) 10314–10321.
[127] Y. Xing, E.W. Ma, K.L. Tsui, M. Pecht, Microelectron. Reliab 53 (2013) 811–820.
[128] M. Zhong, M. Liu, N. Li, X. Bu, J. Energy Chem. 63 (2021) 113–129.
[129] L.M. González, D. Ramirez, F. Jaramillo, J. Energy Chem. 68 (2022) 222–246.
[130] Z. Ji, J. Chen, M. Pérez-Page, Z. Guo, Z. Zhao, R. Cai, M.T.P. Rigby, S.J. Haigh, S.M. Holmes, J. Energy Chem. 68 (2022) 143–153.
[131] Q. Wang, G. Zhang, Y. Li, Z. Hong, D. Wang, S. Shi, npj Comput Mater. 6 (2020) 176.
[132] R. Zhang, X. Shen, Y. Zhang, X. Zhong, H. Ju, T. Huang, X. Chen, J. Zhang, J. Huang, J. Energy Chem. 71 (2022) 29–35.
[133] Y. Kang, L. Li, B. Li, J. Energy Chem. 54 (2021) 72–88.
[134] V. Dao, M. Dinh, C. Kim, M. Park, C. Doh, J. Bae, M. Lee, J. Liu, Z. Bai, Energies. 14 (2021) 2634.

[135] W. Li, I. Demir, D. Cao, D. Jöst, F. Ringbeck, M. Junker, D.U. Sauer, Energy Stor. Mater. 44 (2022) 557–570.

[136] Z. Su, E. Decencière, T.T. Nguyen, NPJ Comput Mater. 8 (2022) 1–11.

[137] H. Zheng, X. Lu, K. He, J. Energy Chem. 68 (2022) 454–493.

[138] X. Chen, X. Liu, X. Shen, Q. Zhang, Angew. Chem. 133 (2021) 24558–24570.

[139] W. Li, N. Sengupta, P. Dechent, D. Howey, A. Annaswamy, D.U. Sauer, J. Power Sources. 482 (2021) 228863.

[140] M. Duquesnoy, T. Lombardo, M. Chouchane, E.N. Primo, A.A. Franco, J. Power Sources. 480 (2020) 229103.

[141] H. Xu, J. Zhu, D.P. Finegan, H. Zhao, X. Lu, W. Li, N. Hoffman, A. Bertei, P. Shearing, M.Z. Bazant, Adv. Energy Mater. 11 (2021) 2003908.